Spontaneous Curvature of Comb Copolymers Strongly Adsorbed at a Flat Interface: A Computer Simulation Study

Johan de Jong,*,† Andrei Subbotin,‡ and Gerrit ten Brinke†

Laboratory of Polymer Chemistry and Materials Science Centre, University of Groningen, Nijenborgh 4, 9747 AG Groningen, The Netherlands, and Institute of Petrochemical Synthesis, Russian Academy of Sciences, Moscow 119991, Russia

Received March 23, 2005; Revised Manuscript Received May 19, 2005

ABSTRACT: Using a modified bond fluctuation model, with only excluded-volume interactions, we demonstrate spontaneous curvature of 2D comb copolymer molecules, provided the side chains are allowed to flip from one side of the backbone to the other. When the side chains are not allowed to flip, the polymer conformations are very stiff. Once flipping is allowed, the polymers display a distinct curvature. We illustrate the curvature by presenting randomly selected snapshots. In addition, bond angle correlation analysis shows that in this case the polymer does not behave like a persistent wormlike chain. In connection to this we outline a model that incorporates curvature and is able to fit the correlation data. Further evidence for spontaneous curvature is given by scattering data displaying a pronounced peak that can be connected to conformational characteristics. Our findings are in good agreement with recent theoretical and experimental studies.

1. Introduction

The conformational properties of comb copolymers consisting of a flexible backbone to which side chains are densely grafted at regular distances have formed the subject of many publications in the past decade.[1−33] The interest arises from the competition between the intrinsic flexibility and the stiffening due to the excluded-volume effect between the side chains. The theoretical papers by Birshtein et al.[1] and Fredrickson[3] laid the foundation for most of the work that followed. The experimental work got going only after suitable polymerization procedures were developed by Schmidt and Tsukahara.[4−6] Experimentally, the main conclusion by Fredrickson that the presence of a dense set of flexible side chains will give rise to shape-persistent cylindrical objects was confirmed by light scattering experiments.[13] The analysis also clearly confirmed the fact that the polymer backbone is far from fully stretched, something that was very obvious from our computer simulations.[14]

From the start, atomic force microscopy (AFM) formed one of the preferred techniques to study individual comb copolymer brush molecules.[21,22,24,25,32] As far as the dilute solution properties are concerned, AFM presents us with an essential problem since the shape of the brush molecules is largely determined by the excluded-volume effect between the side chains, which is obviously much larger in 2D than in 3D. Nevertheless, the main conclusions (e.g., the far from stretched backbone) were readily confirmed.

However, apart from the straight cylinder-like objects theoretically predicted for the 3D conformation of the brush molecules, spiral conformations were also observed.[21] Inspired by these observations, the conformational properties of comb copolymers at a flat surface or interface became a specific area of interest. The first computer simulations in this area, using side chains that were either alternatingly pointing to different sides of the backbone or were allowed to flip freely, just showed persistent cylinder-like objects with a substantial larger persistence length than the corresponding 3D molecules.[13] Both a theoretical analysis and computer simulations demonstrated that a frozen-in uneven distribution of side chains to both sides of the backbone leads to spiral conformations.[21,26] Most excitingly, it was recently observed experimentally that spontaneous curvature may actually already occur when the side chains are simply allowed to traverse freely from one side of the backbone to the other. A subsequent theoretical analysis predicted that in this case straight conformations are indeed unstable with respect to bending.[31,32]

The object of the present study is to investigate the bending instability using a Monte Carlo simulation technique, which does not suffer from the practical problems related to side-chain flipping associated with experiments. The following argument shows that it is also of direct interest for the theoretical analysis. According to the theory for 3D comb copolymer brushes, the presence of the side chains results in a persistent object for which the ratio of the persistence length over the diameter increases strongly with side chain length at fixed grafting density. However, computer simulations have still not been able to confirm this, despite the large size of the molecules studied.[14] Apparently, much larger molecules, molecules outside the realm of present computational possibilities, are required. This observation together with the fact that previous simulations on 2D comb copolymer brushes with flipping of side chains allowed did not reveal any signs of spontaneous curvature suggests that again unrealistically large structures may be required to actually verify the theoretical bending instability prediction.

It turns out that this is not the case. We will show that, when side-chain flipping is allowed, an asymmetric distribution of side chains is indeed favored over a symmetric distribution and that this leads to curvature. Straight conformations with a symmetric distribution

† University of Groningen.
‡ Russian Academy of Sciences.
* Corresponding author: Fax +31 (0)50 363 4400; e-mail jdejong@rug.nl.

10.1021/ma050612+ CCC: $30.25
Published on Web 06/21/2005

of side chains are unstable with respect to bending. In addition, we show that when flipping is allowed the comb copolymer can no longer be described as merely a wormlike chain characterized by a certain persistence length, thus lending more support to the idea that spontaneous curvature is involved. In connection to this we outline a model that incorporates curvature and which is able to fit the correlation data. The persistence length is used as one of the fitting parameters; it is a striking observation that it is not only an order of magnitude smaller when flipping is allowed, but also it is close to both the value of the mean curvature radius and the persistence length in the 3D case. Furthermore, backbone 2D scattering data show a distinct scattering peak, not present when flipping is not allowed, that is consistent with the correlation data and matches visual characteristics of typical snapshots.

2. Model and Methods

2.1. Simulation Model. The simulations were performed using a customized bond fluctuation model[34−37] (BFM) in two dimensions. In the BFM a polymer chain, consisting of any number of beads, resides on a square lattice. Every bead occupies 2^D lattice sites, with D denoting the number of dimensions.

During simulation the bond length is allowed to vary. For $2D$ systems the original set of bond vectors are those with lengths $b \in [2, \sqrt{13}]$.[34] The Monte Carlo sampling scheme in the context of the BFM consists of repeatedly choosing a random bead in the system and attempting to displace it by one lattice spacing in a randomly chosen direction along the principal axes. The move is rejected if the resulting system either violates excluded-volume or bond length restrictions. If the system incorporates interactions, the transition probability is furthermore determined by applying the Metropolis criterion. The initial system is equilibrated by applying the BFM scheme until collective properties of the system start oscillating around a certain constant value. In relation to this it is important to check that independent simulations with different starting conditions (e.g., starting conformation) equilibrate toward the same free energy minimum to exclude the possibility of getting stuck in a local minimum. Physical quantities of interest in equilibrium may then be calculated by simple averaging over all sampled states of the system. To check whether sufficient statistical power has been obtained, a time correlation analysis is performed in accordance with Flyvbjerg and Petersen.[38]

The simulations are performed on an "infinite" two-dimensional square lattice, as opposed to imposing periodic boundary conditions.[33] This is advantageous when simulating single polymer chains. Usually, as for simulations of polymer melts, a finite lattice is used with periodic boundary conditions. Always precautions have to be taken to ensure that monomers of a given chain do not interact with monomers of a different periodic image. This implies a simulation box that is considerably larger than the polymer chain itself, resulting in extreme memory requirements for large polymer chains.

The two-dimensional lattice as present in computer memory consists of 200×200 lattice sites. These are mapped onto the bead position vectors $\{\vec{r} = (x, y) | 0 \le x, y < 200\}$. Position vectors outside this region are mapped back into the finite lattice, preserving their "real" coordinate in memory as well. Effectively, a list (which may be empty) of beads is connected to each lattice site in the finite lattice, with monomers in the list belonging to different, nonoverlapping, regions in real lattice space. In fact, it is like folding a road map with the size of the map growing and shrinking as required. The main advantage of this technique is that, as far as the polymer chain is concerned, the lattice has infinite size, and undesirable interactions between periodic images are prevented independent of the size of the finite lattice in computer memory.

Restricting the size of the finite lattice to 10×10 does not have any influence on the results (the set of samples of the system is independent of the size of the finite lattice) of the simulation except for an efficiency penalty. This makes it possible to perform simulations of large systems even when memory restrictions are tight. The benefit of our approach is even more apparent for 3D simulations.

For the systems under consideration no interactions were present except for excluded volume. We consider two particular systems. The first system is a comb copolymer with evenly and symmetrically distributed side chains. In the second system the side chains are allowed to flip from one side of the backbone to the other. To realize the possibility of flipping, we introduce a nonstandard BFM move that flips one side chain and its grafting point on the backbone in its entirety. As the BFM involves a lattice, the transformation should map lattice sites onto lattice sites. In addition, the acceptance ratio is increased and the computational effort decreased when the transformation conserves distance and consequently bond length. A parallelogram construction incorporates these prerequisites and necessitates merely vector addition. Specifically, the parallelogram consists of the two backbone beads neighboring the grafting point, a bead to be moved and the new position of the bead, where the backbone beads are on opposite corners. Flipping a side chain may result in bond crossing and entangling of side chains. Since our objective is to address the theoretical predictions, a strict 2D system is simulated in which bonds may not cross. In fact, in the original description of the 2D BFM model this very restriction led to the set of allowed bond vectors.[34] Therefore, it is important to check for its occurrence and to reject the move accordingly. The simulation proceeds in such a way that there is a considerably smaller probability for flipping trial moves than for standard BFM moves.

Since the systems in our present study are very densely grafted, the 2D conformations are highly stretched. This may lead to so-called quasi-nonergodicity on a lattice as grafts are partially "trapped". Extremely large simulation times are required for good statistics indicated by e.g. plateaus in simulation data with high correlation times and an an absence of any rotational diffusion, especially for the nonflipping case. The problem can solved by introducing nonlocal trial moves. We have chosen to employ the so-called "shift move". A random backbone bead is selected. Just as in the case of local moves the trial move displaces the bead by one lattice spacing. However, in this case the part of the backbone on one of the sides of the selected bead is moved in the same way, together with all attached side chains. The shift move is of the order of $N_{\text{backbone}}/4$ times more efficient in relaxing the backbone. As the grafts (backbone) are not partially trapped anymore, the ergodicity problems vanish.

2.2. Analysis. The data were analyzed by evaluating a bond angle correlation plot. For simple persistent wormlike chains it holds that $\langle \cos \theta(s) \rangle \propto \exp(-s/\lambda)$. Here $\cos \theta(s)$ is the cosine of the angle between two tangents to the backbone that are s monomers apart. The brackets denote a thermodynamic average. In other words, a plot of the logarithm of $\langle \cos \theta(s) \rangle$ vs s should yield a straight line with a slope equal to minus the inverse of the persistence length. However, for an object that is either nonpersistent or involves not only a persistent mechanism, such as in the case of spontaneous curvature, the plot will not exhibit linear behavior.[39]

The track of a Brownian particle simulates a linear polymer.[40,41] Therefore, the two-point probability distribution satisfies a Fokker−Planck equation.[41−43] We incorporate bending by including an external potential that is perpendicular to the track of the Brownian particle. The bending elasticity (persistence) turns up as the inverse of the diffusion coefficient and so

$$\frac{\partial \psi}{\partial s} = \frac{1}{\lambda} \Delta_n \psi + \nabla_n (\nabla_n U \psi) \tag{1}$$

Here $\psi(s,\vec{r})$ is the distribution function for the tangent to the chain, s is the contour parameter along the chain, and $U(\vec{r})$ is the external potential. Since bending occurs in the plane, it reduces to a one-dimensional problem ($\Delta_n = \partial^2/\partial\theta^2$).[43,44] The potential is analogous to a constant centrifugal force; therefore, the second derivative vanishes, and the direction is along the polar angle

$$\frac{\partial \psi}{\partial s} = \frac{1}{\lambda} \frac{\partial^2 \psi}{\partial \theta^2} + C \frac{\partial \psi}{\partial \theta} \tag{2}$$

Here C is the curvature (strength of the potential). The quantity we are interested in is defined as

$$\mu(s) = \left\langle \left(\frac{\partial \vec{r}}{\partial s}\right)_p \cdot \left(\frac{\partial \vec{r}}{\partial s}\right)_{p+s} \right\rangle_{p,\alpha} = \left\langle \left(\frac{\partial \vec{r}}{\partial s}\right)_0 \cdot \left(\frac{\partial \vec{r}}{\partial s}\right)_s \right\rangle_{\alpha} = \langle \cos \theta(s) \rangle = \int_0^{2\pi} \psi(s,\theta) \cos \theta \, \mathrm{d}\theta \tag{3}$$

where α denotes averaging over conformations. Similarly, we can define $\nu(s)$ for the sine instead of the cosine. Upon multiplying (2) with $\cos \theta$, integrating over θ, and repeating the procedure for $\sin \theta$, the original equation is written as a system of two coupled differential equations. For $\mu(s)$ the system yields

$$\mu'' + \frac{2}{\lambda} \mu' + \left(C^2 + \frac{1}{\lambda^2}\right) \mu = 0 \tag{4}$$

which has a solution of the form

$$\mu(s) = \langle \cos \theta(s) \rangle = \int_0^{2\pi} \mathrm{d}\theta \, \psi(s,\theta) \cos \theta = \mathrm{e}^{-s/\lambda} \cos(Cs) \tag{5}$$

Note that in the absence of curvature (i.e., $C = 0$) the result for a simple persistent wormlike chain is retained. In addition, for a fully persistent chain ($\lambda \to \infty$) the result for a perfect ring with radius $R = 1/C$ is obtained.

Information on the conformational properties of single polymer chains can also be obtained from the experimentally accessible form factor or scattering function, which involves the Fourier transform of the density profile and is defined as

$$S(\vec{q}) = \frac{1}{M} \left| \int_V \mathrm{d}V \rho(\vec{r}) \mathrm{e}^{i\vec{q}\vec{r}} \right|^2 \tag{6}$$

with M the total mass, or equivalently for the discrete case such as in simulation studies

$$S(\vec{q}) = \frac{1}{N} \left\langle \left| \sum_{i=0}^{N-1} \mathrm{e}^{i\vec{q}\vec{r}_i} \right|^2 \right\rangle \tag{7}$$

from this the form factor is obtained by averaging over q-vectors with the same length.

For persistent self-avoiding walks (SAW's) the form factor behaves as $q^{1/\nu}$ at intermediate values of q, where ν is the scaling exponent for the SAW (3/4 in 2D). For large values of q ($q\lambda \gg 2\pi$), $S(q)$ behaves as q^{-1}, which is the so-called rigid-rod regime; i.e., at very small length scales the chain is a stiff object. However, for chains that exhibit curvature the form factor may show distinct peaks for certain characteristic length scales as will be discussed in more detail in the results.

In a Holtzer plot $qS(q)$ is plotted vs q, and the plot reaches a horizontal plateau in the rigid-rod regime. It is well-known that the height of the plateau equals πM_L, where M_L is the linear mass density.[28,45,46] Therefore, a Holtzer plot provides direct information on the amount of stretching of the backbone of a comb copolymer chain. Since the mass of all backbone beads equals unity, the height of the Holtzer plateau equals π/l, where l is the contour length per segment that can be compared to the mean bond length $\langle b \rangle$.

In 2D the situation is slightly different. In the present study 2D scattering is calculated; i.e., all q-vectors are in the plane of the chain conformation. It can be shown that in this case the height of the Holtzer plateau equals $2/l$, and a sketch of the derivation is provided in the Appendix.

3. Results and Discussion

Two different architectures were studied using the methods described in the previous section. The first system consists of a backbone of 100 segments, to each of which a side chain is grafted with a length equal to 10 segments. This system was studied in three different cases.

To compare the 2D behavior to the 3D behavior, athermal simulations of the comb copolymer brush were performed in dilute solution. The BFM in the 3D case is similar to the 2D version, the main difference being the allowed set of bond lengths: $b \in \{2, \sqrt{5}, \sqrt{6}, 3, \sqrt{10}\}$.[33,36,37] The remaining two cases are both 2D. The difference between the two is whether or not the side chains are allowed to flip from one side of the backbone to the other side.

The 2D system with flipping not allowed started out as a straight backbone with side chains alternatingly pointing out to both sides of the backbone. A total number of 6000 samples were obtained at regular intervals of 100 000 MC moves. The ratio of local moves to shift moves was 1:5000, and the acceptance ratio of the shift moves equal to 0.19, which is nearly half that of the local moves.

In the case with flipping allowed, systems starting out with all side chains pointing out to the same side as well as symmetric systems have been equilibrated. Using the same interval as in the symmetric case, 40 000 samples were obtained. The acceptance ratio of

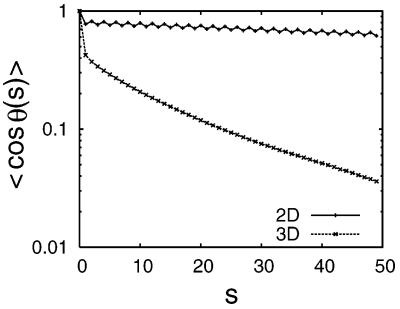

Figure 1. Bond angle correlation plot for the same comb copolymer brush in 2D and 3D. It consists of a backbone of 100 segments, to each of which a side chain of length 10 segments is grafted. s denotes the distance in segments along the chain, and the y-axis denotes the thermodynamic average of the cosine of the angle between two tangents to the backbone that are s beads apart. $\lambda_{3D} \approx 25$ segments and $\lambda_{2D} \approx 211$ segments. Note that the 2D system displays a zigzag effect due to the regularity of the side chain grafting, since flipping is not allowed.

the shift moves dropped to 0.16. In addition to the local and shift moves, flip moves were performed at a ratio of 1:2000 with respect to local moves. The acceptance ratio of the flip moves equaled 0.000 43, explaining the longer simulation times required to obtain good statistics.

The second system was comb copolymer brush consisting of a backbone of 250 segments and side chains of length 5. This system was studied only in the case that flipping is allowed. A total number of 2000 samples was obtained at intervals of 100 000 MC moves. Since the side chain lengths were shorter in this case, the acceptance ratio of the nonlocal moves was higher: 0.24 for shift moves and 0.012 for the flip moves. Because of the strong dependence on the side chain length, it may not be feasible to investigate systems with side chains longer than 20 in this way.

Figure 1 shows the bond angle correlation plot for the system with a backbone length of 100 segments both in the 2D (no flipping) and 3D case. It is immediately apparent that there is more than a factor of 8 between the respective persistence lengths. For the 2D system a pronounced zigzag effect is present. This is due to the fact that the side chains are grafted alternatingly along the backbone. It has a measurable mean effect of displacing the odd numbered beads with respect to the even number beads. In fact, both sides of the comb repel each other because of an excluded-volume effect that is averaged out in the 3D case. Since in the 3D case the comb copolymer is very flexible, the bond angle correlation plot does not satisfy a linear relation for small s. This will turn up again in the discussion of Holtzer plots. To remove end effects, because of the increased flexibility of the ends of the combs, 10 backbone beads at the ends have been excluded from each calculation.

When flipping is allowed for the 2D system, the behavior is entirely different. Figure 2 displays the bond angle correlation plot in this case. Here the data are not presented on a logarithmic scale since for a wide range of s values the result is negative. Apparently, tangents to the backbone at a distance of 24 beads apart are, taken on the mean, perpendicular. A theoretical fit of the curve is displayed as well. For small values of s the theoretical curve fits quite well, but for larger values of s the fit becomes increasingly worse. Nevertheless, it is clear that Figure 2 does not show the behavior of a

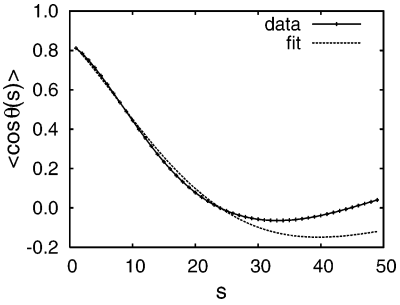

Figure 2. Bond angle correlation plot for a 2D comb copolymer brush with flipping allowed. The backbone length is 100 segments and the side chain length 10 segments. The dashed line is a theoretical fit with parameters $\lambda \approx 25$ segments and a radius of curvature $R \approx 15$ segments.

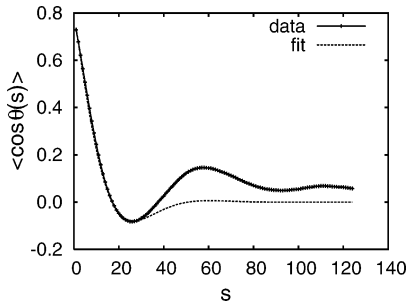

Figure 3. Bond angle correlation plot for a 2D comb copolymer brush with flipping allowed. The backbone length is 250 segments and the side chain length 5 segments. The dashed line is a theoretical fit with parameters $\lambda \approx 13$ segments and a radius of curvature $R \approx 11$ segments.

wormlike chain and is strongly indicative of an existing mean curvature.

In the case of the 250 × 5 system the curvature is even more pronounced. The bond angle correlation plot for this system is shown in Figure 3. As expected, the persistence length obtained by fitting the data with a theoretical curve is much smaller in this case. The effect on the fitted radius of curvature is less pronounced. However, since the ratio between the backbone length and the curvature radius (as well as the persistence length) is more than a factor of 3 greater here, the chain is possibly meeting itself more often and is therefore experiencing a greater excluded-volume effect. On the other hand, if the side chains obey SAW statistics, the result is in agreement with the theoretical prediction that the curvature radius is proportional to the side chain mean end to end distance.[32]

For small values of s the theoretical curve fits very well. As before, the theoretical fit becomes worse for large values of s. Moreover, because of the cosine term in our theoretical result, the first two zeros should be at a 1:3 ratio, which is clearly not the case. This is to be expected, however, if the sign of the curvature is not constant along the backbone, which is an implicit assumption in our theoretical model. A certain analogy to the one-dimensional Ising model is present. There is no reason for a net mean curvature to exist and no mechanism present to break the symmetry, although the existence of domains with constant (sign of) curvature is possible.

Another method that may reveal any present mean curvature effect is by calculating the form factor as this involves the Fourier transform of the density profile. In the case of a perfect ring in 2D for example, the analytical result involves the square of a Bessel function

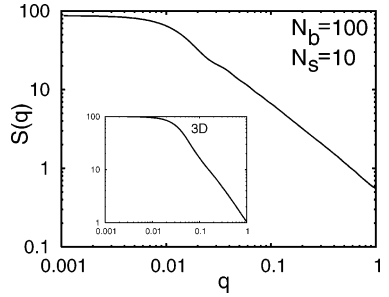

Figure 4. Scattering plot for the 2D comb copolymer brush with backbone length 100. Flipping is not allowed. Inset: scattering plot in dilute solution.

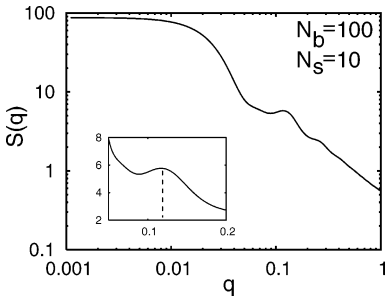

Figure 5. Scattering plot for the 2D comb copolymer brush with backbone length 100 and side chain length 10. Flipping is allowed. Note that it shows a distinct peak near $q = 0.12$ as well as a weaker second peak near $q = 0.25$. Inset: enlargement on a linear scale of the scattering plot near the first peak.

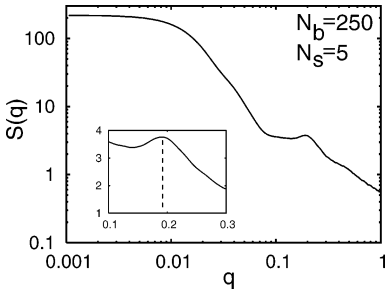

Figure 6. Scattering plot for the 2D comb copolymer brush with backbone length 250 and side chain length 5. Flipping is allowed. Note that it shows a distinct peak near $q = 0.2$. Inset: enlargement on a linear scale of the scattering plot near the peak.

of the first kind, $S(q) \propto RJ_0^2(qR)$. In this case the scattering function shows distinct minima and maxima, and the first maximum corresponds to a length scale in the order of the ring diameter.

Figure 4 shows the 2D scattering result on the 2D system for which flipping is not allowed. The scattering behavior is quit similar to what is known for the 3D case as shown, e.g., in the inset. However, when flipping is allowed, the behavior is again quite different as demonstrated by Figure 5. Most strikingly, the scattering displays a distinct peak that may be indicative of some characteristic length scale.

For the 250 × 5 system, the situation is similar. A scattering plot is shown in Figure 6. Also in this case the scattering exhibits a distinct peak, but here belonging to a smaller length scale.

The presence of a spontaneous curvature as indicated by the bond angle correlation plots as well as the scattering plots should be discernible visually as well. Figure 7 presents a typical snapshot for the 100 × 10 system for which flipping is not allowed. The comb copolymer appears to be very stiff, which should not come as a surprise since the backbone length is less than half the persistence length. As the side chains have no way to travel from one side of the backbone to the other side, the side chain distribution is perfectly symmetric.

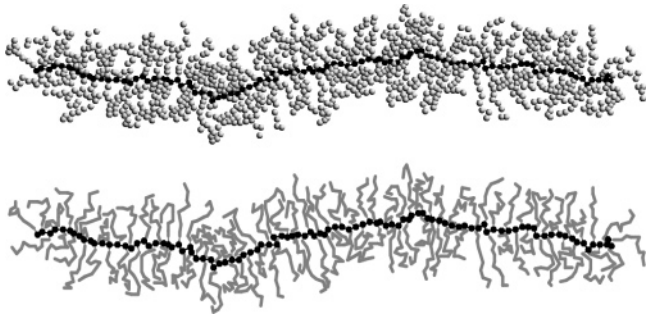

Figure 7. Typical snapshot of the 2D comb copolymer brush with backbone length 100 and side chain length 10 when flipping is not allowed. The comb copolymer appears to be very stiff. The bottom part shows an alternative view that allows for seeing the side chain trajectories more easily.

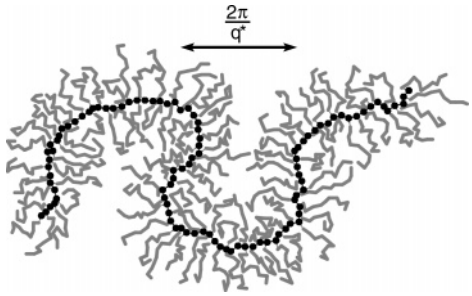

Figure 8. Typical snapshot of the 2D comb copolymer brush with backbone length 100 and side chain length 10 when flipping is allowed. In this case the conformation has assumed a strongly curved shape although the backbone still appears rather stretched. Note that the side chain distribution locally is distinctly asymmetric. The arrow indicates the length scale belonging to the scattering peak in Figure 5.

As is clear from Figure 8, the conformational characteristics are quite different when flipping is allowed. The typical snapshot displayed here exhibits a pronounced curvature. It appears that the backbone is still rather stretched, but the side chain distribution locally shows a distinct asymmetry. Although Figure 8 shows a randomly selected snapshot, its characteristics can be brought into agreement with Figure 2. The length scale belonging to the scattering peak in Figure 5 is indicated by an arrow in Figure 8. Care must be taken not to draw too many conclusions from just one snapshot. However, the conformation is consistent with the scattering data in the sense that it is possible that the indicated length scale corresponds to the magnitude of some mean curvature radius on intermediate length scales. A selection of snapshots is displayed in Figure 9, showing among others meandering conformations and horseshoe-like conformations.

A typical snapshot of the 250 × 5 system is presented in Figure 10. The strongly curved shape is even more indicative of spontaneous curvature than for the 100 × 10 system. The arrow indicates the length scale belonging to the scattering peak in Figure 3. Also in this case, the conformational behavior of the snapshot is consistent with both the bond angle correlation plot and the scattering.

The snapshots suggest that the curvature is due to local deviations from a symmetric distribution of side

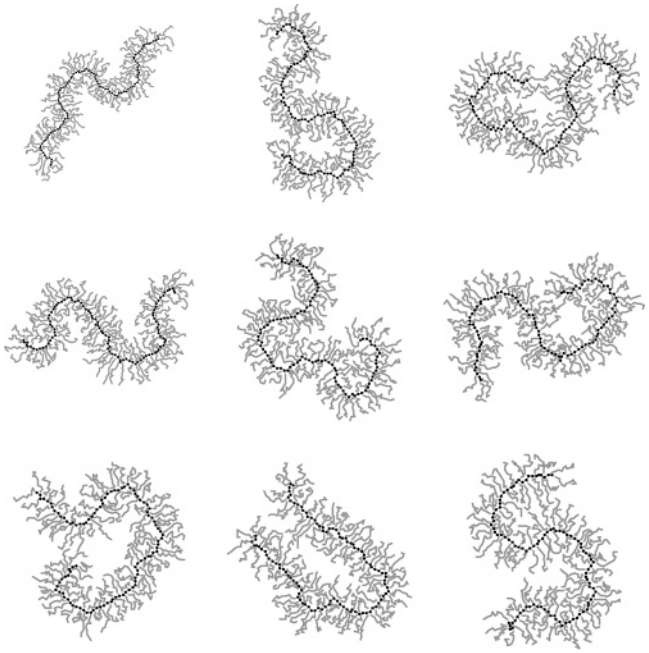

Figure 9. An assortment of snapshots for the 2D system with backbone length 100 and side chain length 10 when flipping is allowed. All conformations display a strongly curved shape, and meandering chains as well as horseshoe-like conformations are present.

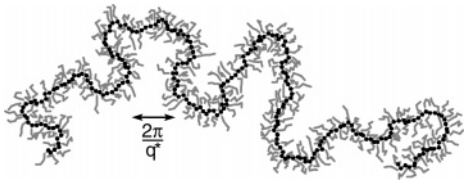

Figure 10. Typical snapshot of the 2D comb copolymer brush with backbone length 250 and side chain length 5 when flipping is allowed. In this case the conformation has assumed a strongly curved shape although the backbone still appears rather stretched. Note that the side chain distribution locally is distinctly asymmetric. The arrow indicates the length scale belonging to the scattering peak in Figure 6.

chains with respect to the backbone and thus in excellent agreement with the recent theoretical treatments of the "flipping" case that demonstrated a lowering of the free energy when the side chains are distributed asymmetrically.[21,26,31,32] If flipping is allowed, it is thermodynamically more favorable for the backbone to show meandering behavior. When simulating systems without interactions, the lowering of the free energy is entirely due to the increase of entropy.

Figure 11 presents a Holtzer plot for the 100 × 10 2D comb copolymer brush. The height of the Holtzer plateau indicates a contour length per segment $l = 3.0$ that is only slightly smaller than the mean bond length $\langle b \rangle = 3.19$. This means that the backbone is rather stretched, a fact that agrees with visual inspection of the snapshot. In the case that flipping is allowed, the Holtzer plot does not seem to reach a plateau, as is demonstrated by the inset of Figure 11. For values of q larger than displayed here the plot appears to level out to ~0.6. However, the range of q values already goes beyond the start of the persistent regime as estimated by the fit of the bond correlation plot. In addition, the value of 0.6 for the height of the plateau corresponds to a contour length per segment that is larger than the mean bond length, which is clearly impossible. We

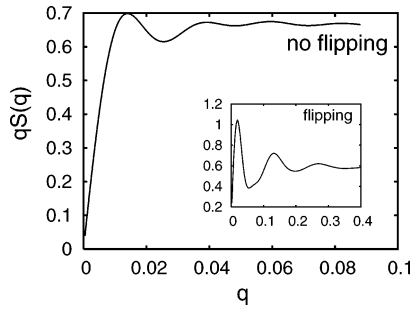

Figure 11. Holtzer plot of the 2D comb copolymer brush with length 100 and side chain length 10 when flipping is not allowed. In 2D there is a decaying oscillation for a rigid rod (see Appendix) that is also present here. The height of the horizontal Holtzer plateau is ~0.67, which corresponds to a contour length per segment of 3.0 lattice spacings which is only slightly smaller than the mean bond length $\langle b \rangle = 3.19$. Inset: Holtzer plot for the case when flipping is allowed. No Holtzer plateau is reached, and the plot appears to level out to ~0.6 which would indicate a contour length per segment larger than the mean bond length; i.e., no rigid-rod regime can be discerned.

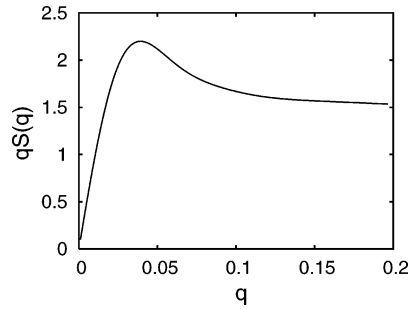

Figure 12. Holtzer plot of the 3D comb copolymer brush with length 100 and side chain length 10. For very flexible chains the Holtzer plot does not level off completely, but taking a value of 1.5 for the Holtzer plateau provides a upper estimate for the contour length per segment of 2.1, which is distinctly smaller than the mean bond length $\langle b \rangle = 2.8$.

conclude that no rigid-rod regime can be discerned in the case of spontaneous curvature.

Since the backbone is very stretched, it may be expected that a good estimate on the contour length per segment is obtained by assuming an all-trans arrangement of the segments and calculating l from the mean cosine between bond angles and the mean bond length. The values for the nonflipping case are $\langle \cos \theta(1) \rangle \approx 0.774$ and $\langle b \rangle \approx 3.19$, from which we calculate $l \approx 3.0$, consistent with the Holtzer plot data. For the flipping case $\langle \cos \theta(1) \rangle \approx 0.809$ and $\langle b \rangle \approx 3.23$, giving $l \approx 3.1$. The amount of stretching remains almost unchanged, and the small difference may be explained by the same even−odd effect in the nonflipping case that also gave rise to the zigzag effect in the bond angle correlation plot of the nonflipping case.

For comparison, the Holtzer plot of the 3D comb copolymer brush in dilute solvent is shown in Figure 12. In this case the polymer is very flexible, and for this reason the Holtzer plot never completely levels out to a horizontal plateau. However, a contour length per segment $l \approx 2.1$ can be estimated that is significantly smaller than the mean bond length $\langle b \rangle = 2.8$. Clearly, the backbone is far from completely stretched.

These results demonstrate that the curved conformations observed in recent experiments[25,32,47] may indeed be due to a spontaneous occurring asymmetric distribution of side chains. Also, using detailed snapshots, the

interplay between curvature and asymmetric distribution of side chains is effectively illustrated.

The fact that the "nonflipping" comb appears much more stiff than in the 3D case is consistent with the findings of Saariaho et al.[13] In that study the side chains were allowed to flip. However, no pronounced curvature was found, and the qualitative behavior of the 2D comb was more similar to the "nonflipping" case in the present study. We would like to stress the fact that the grafting density is twice as high in the present study.

The influence of grafting density and the side chain parameters needs to be examined in more detail, and a more exhaustive study will be presented in a future publication.

4. Concluding Remarks

Using a custom bond fluctuation model, we examined curvature in 2D comb copolymer brushes. We were able to demonstrate that when the side chains are allowed to flip from one side to the other side of the backbone, the system displays spontaneous curvature. Moreover, we confirmed that this curvature is the result of an asymmetric distribution of side chains and that this is favorable to a symmetric distribution; i.e., when flipping is allowed, the system is unstable with respect to bending, resulting in observed meandering or horseshoe-like conformations. The visual evidence for spontaneous curvature to occur is supported by the analysis of the bond angle correlation as well as scattering analysis. In addition, Holtzer analysis indicates also that the system, when flipping is allowed, does not behave like a simple persistent (wormlike) chain.

We have outlined a theoretical model, including both persistence and curvature, with which it is possible to fit the correlation plot. The fact that spontaneous curvature did not turn up in previous simulation studies (Saariaho et al.[13]) may be attributed to the lower grafting density of side chains when compared to the present study. Comparison with the dilute solution case shows, that when flipping is allowed, the persistence length drops to the order of magnitude of the 3D case.

By showing that relatively short side chains already give rise to spontaneous curvature, we demonstrate the importance of this observation for experimental systems. In connection with this it is of interest to note that simulations on three-dimensional comb copolymer brushes have failed so far to confirm the theoretical prediction that the persistence length λ divided by the diameter D of the brush increases almost linearly with side chain length for a given grafting density.[3,19] In fact, all that the simulations demonstrate is that this ratio λ/D remains constant at best (decreases slightly). Apparently extremely large structures are required to enter the regime where this prediction holds. That this is not the case here is an important result.

Acknowledgment. A. Subbotin acknowledges financial support from Netherlands Organisation for Scientific Research (NWO) within the Dutch Russian scientific cooperation program.

Appendix. 2D Scattering from a Rigid Rod

The scattering function for a 2D rigid rod with linear density ρ and length l equals (eq 6)

$$S(\vec{q}) = \frac{1}{l\rho}\left|\int_{-l/2}^{l/2} \mathrm{d}x\ \rho \mathrm{e}^{iqx\cos\theta}\right|^2 = \rho l\left(\frac{\sin((ql\cos\theta)/2)}{(ql\cos\theta)/2}\right)^2 \quad (8)$$

where θ is the angle between $\vec{q}$ and the rod. The form factor is obtained by averaging over all orientations of $\vec{q}$ (no azimutal angle as in the case of 3D) and for the Holtzer plateau

$$H = \lim_{\hat{q}\to\infty} \frac{2\rho}{\pi\hat{q}} \int_0^{\pi} \mathrm{d}\theta \left(\frac{\sin(\hat{q}\cos\theta)}{\cos\theta}\right)^2 = \lim_{\hat{q}\to\infty} \frac{2\rho}{\pi\hat{q}} I(\hat{q}) \quad (9)$$

The integral $I(\hat{q})$ can be evaluated by taking the derivative with respect to $\hat{q}$ and integrating $I'(\hat{q})$ in the complex plane using a suitable reparametrization. The boundary condition $H(0) = 0$ finally yields $H = 2\rho$.

References and Notes

(1) Birshtein, T.; Borisov, O.; Zhulina, Y.; Khokhlov, A.; Yurasova, T. *Polymer Sci. USSR* **1987**, *29*, 1293.
(2) Wang, Z.; Safran, S. *J. Chem. Phys.* **1988**, *89*, 5323.
(3) Fredrickson, G. *Macromolecules* **1993**, *26*, 2825.
(4) Wintermantel, M.; Schmidt, M.; Tsukahara, Y.; Kajiwara, K.; Kohjiya, S. *Macromol. Rapid Commun.* **1994**, *15*, 279.
(5) Wintermantel, M.; Fischer, K.; Gerle, M.; Ries, R.; Schmidt, M.; Kajiwara, K.; Urakawa, H.; Wataoka, I. *Angew. Chem., Int. Ed. Engl.* **1995**, *34*, 1472.
(6) Wintermantel, M.; Gerle, M.; Fischer, K.; Schmidt, M.; Wataoka, I.; Urakawa, H.; Kajiwara, K.; Tsukahara, Y. *Macromolecules* **1996**, *29*, 978.
(7) Dziezok, P.; Sheiko, S.; Fischer, K.; Schmidt, M.; Möller, M. *Angew. Chem., Int. Ed. Engl.* **1997**, *36*, 2812.
(8) Sheiko, S.; Gerle, M.; Fischer, K.; Schmidt, M.; Möller, M. *Langmuir* **1997**, *13*, 5368.
(9) Saariaho, M.; Ikkala, O.; Szleifer, I.; Erukhimovich, I.; ten Brinke, G. *J. Chem. Phys.* **1997**, *107*, 3267.
(10) Ten Brinke, G.; Ikkala, O. *Trends Polym. Sci.* **1997**, *5*, 213.
(11) Saariaho, M.; Szleifer, I.; Ikkala, O.; ten Brinke, G. *Macromol. Theory Simul.* **1998**, *7*, 211.
(12) Rouault, Y. *Macromol. Theory Simul.* **1998**, *7*, 359.
(13) Saariaho, M.; Ikkala, O.; ten Brinke, G. *J. Chem. Phys.* **1999**, *110*, 1180.
(14) Saariaho, M.; Subbotin, A.; Szleifer, I.; Ikkala, O.; ten Brinke, G. *Macromolecules* **1999**, *32*, 4439.
(15) Gerle, M.; Fischer, K.; Roos, S.; Müller, A.; Schmidt, M.; Sheiko, S.; Prokhorova, S.; Möller, M. *Macromolecules* **1999**, *32*, 2629.
(16) Fischer, K.; Gerle, M.; Schmidt, M. *Proc. ACS PMSE Anaheim* **1999**, *30*, 133.
(17) Saariaho, M.; Subbotin, A.; Ikkala, O.; ten Brinke, G. *Macromol. Rapid Commun.* **2000**, *21*, 110.
(18) Khalatur, P. G.; Shirvanyanz, D. G.; Starovoitova, N. Y.; Khokhlov, A. R. *Macromol. Theory Simul.* **2000**, *9*, 141.
(19) Subbotin, A.; Saariaho, M.; Ikkala, O.; ten Brinke, G. *Macromolecules* **2000**, *33*, 3447.
(20) Subbotin, A.; Saariaho, M.; Ikkala, O.; ten Brinke, G. *Macromolecules* **2000**, *33*, 6168.
(21) Khalatur, P. G.; Khokhlov, A. R.; Prokhorova, S. A.; Sheiko, S. S.; Möller, M.; Reineker, P.; Shirvanyanz, D. G.; Starovoitova, N. *Eur. Phys. J. E* **2000**, *1*, 99.
(22) Prokhorova, S.; Sheiko, S.; Mourran, A.; Azumi, R.; Beginn, U.; Zipp, G.; Ahn, C.; Holerca, M.; Percec, V.; Möller, M. *Langmuir* **2000**, *16*, 6862.
(23) Sheiko, S. *Adv. Polym. Sci.* **2000**, *151*, 61.
(24) Sheiko, S.; Möller, M. *Chem. Rev.* **2001**, *101*, 4099.
(25) Sheiko, S.; Prokhorova, S.; Beers, K.; Matyjaszewski, K.; Potemkin, I.; Khokhlov, A.; Möller, M. *Macromolecules* **2001**, *34*, 8354.
(26) Potemkin, I.; Khokhlov, A.; Reineker, P. *Eur. Phys. J. E* **2001**, *4*, 93.
(27) Stepanyan, R.; Subbotin, A.; ten Brinke, G. *Phys. Rev. E* **2001**, *63*, 61805.
(28) Fischer, K.; Schmidt, M. *Macromol. Rapid Commun.* **2001**, *22*, 787.
(29) Stepanyan, R. R.; Subbotin, A.; ten Brinke, G. *Macromolecules* **2002**, *35*, 5640.
(30) Flikkema, E.; ten Brinke, G. *Macromol. Theory Simul.* **2002**, *11*, 777.
(31) Potemkin, I. *Eur. Phys. J. E* **2003**, *12*, 207.
(32) Potemkin, I.; Khokhlov, A.; Prokhorova, S.; Sheiko, S.; Möller, M.; Beers, K.; Matyjaszewski, K. *Macromolecules* **2004**, *37*, 3918.

(33) de Jong, J.; ten Brinke, G. *Macromol. Theory Simul.* **2004**, *13*, 318.
(34) Carmesin, I.; Kremer, K. *Macromolecules* **1988**, *21*, 2819.
(35) Deutsch, H. P.; Dickman, R. *J. Chem. Phys.* **1990**, *93*, 8983.
(36) Deutsch, H. P.; Binder, K. *J. Chem. Phys.* **1991**, *94*, 2294.
(37) Deutsch, H. P.; Binder, K. *Macromolecules* **1992**, *25*, 6214.
(38) Flyvbjerg, H.; Petersen, H. G. *J. Chem. Phys.* **1989**, *91*, 461.
(39) Flikkema, E.; Subbotin, A.; ten Brinke, G. *J. Chem. Phys.* **2000**, *113*, 7646.
(40) Kuhn, W. *Kolloid-Z.* **1934**, *68*, 2.
(41) Papadopoulos, G.; Thomchick, J. *J. Phys. A: Math. Gen.* **1977**, *10*, 1115.
(42) Freed, K. *J. Chem. Phys.* **1971**, *54*, 1453.
(43) Winkler, R.; Harnau, L.; Reineker, P. *Macromol. Theory Simul.* **1997**, *6*, 1007.
(44) Subbotin, A.; ten Brinke, G.; Kulichikhin, V.; Hadziioannou, G. *J. Chem. Phys.* **1998**, *109*, 827.
(45) Schmidt, M.; Paradossi, G.; Burchard, W. *Macromol. Rapid Commun.* **1985**, *6*, 767.
(46) Schmidt, M.; Stockmayer, W. H. *Macromolecules* **1984**, *17*, 509.
(47) Sheiko, S.; da Silva, M.; Shirvaniants, D.; Rodrigues, C.; Beers, K.; Matyjaszewski, K.; Potemkin, I.; Möller, M. *Polym. Prepr. (Am. Chem. Soc., Div. Polym. Chem.)* **2003**, *44*, 544.

MA050612+